

Sensitivity of wind wave simulation to coupling with a tide/surge model with application to the Southern North Sea

J. Monbaliu*, C.S. Yu[†] and P. Osuna*

Abstract

The wave-current interaction process in a one way coupled system for the Southern North Sea region was studied. To this end, a modified version of the third-generation spectral wave model WAM was run in a three level nested grid system, taking into account the hydrodynamic fields (coupled version) computed by a tide/surge model. The resolution in these three grids corresponds roughly to 35 km (coarse), 5 km (local) and 1 km (fine). Hydrodynamic information was only available at the resolution of the local grid. Results are compared with those of the same version without considering the interaction with tide and surges (uncoupled version). The emphasis is on the results from the local grid calculations. The sensitivity to the source of boundary conditions (coupled vs. uncoupled) and to the frequency of information exchange is investigated. Also the spectral evolution is studied.

Numerical results in the local grid are in good agreement with buoy data. The phase and amplitude of the modulations of wave period observed from the buoy data are quite well reproduced by the coupled version. The model results in the local grid did not show much sensitivity to the source of boundary condition information, nor were they very sensitive to the information update frequency of the hydrodynamic fields. The directional spectra computed in the coupled mode show a broader energy distribution and a more rapid growth. The fine grid results only differ marginally from the local grid results due to the limited resolution of the hydrodynamic fields used.

*Laboratory of Hydraulics, K.U.Leuven, de Croylaan 2, B-3001 Heverlee, Belgium.

[†]Dept. of Marine Env. and Eng., NSYSU, Lien-Hai Road 70, Kaoshiung 804, Taiwan.

1 Introduction

Wind generated waves can be affected considerably when they interact with currents. When waves propagate on an inhomogeneous and unsteady current field, some particular characteristics of the wave signal are modified, e.g. wavelength, amplitude, frequency, direction, etc. A review of the theoretical aspects concerning the wave-current interaction can be found in Jonsson (1990).

In coastal regions with appreciable tide, the varying water depth as well as the varying currents influence the wave pattern. Besides of the current interaction processes, interaction with the bottom introduce a series of linear and non-linear mechanisms in the spectral transformation (Shemdin et al., 1980). According to Graber and Madsen (1988), in finite-depth waters the shape of the spectrum is to a great extent influenced by the bottom friction term.

By coupling a third generation wave model with a two-dimensional or three-dimensional current model, improved estimates of wave parameters or improved estimates of surge levels can be obtained. Improved parameter estimates for wave conditions are, next to a help for safer navigation and design of coastal structures, of considerable interest for the estimation of sediment movement since wave action can determine to a large extent the resuspension, deposition rate, and transport of sediments (Mei et al., 1997). Coupling can be done at different levels of complexity. Complex coupled systems can have dynamic interactions, where changes in one model also affect the processes in the other model(s) and an iterative numerical procedure might become necessary. The simplest configuration is a loose one way coupling where information from one model is transferred to another model. Considerable work has already been done. Two literature examples are given to illustrate the concept. Mastenbroek et al., (1993) studied the effect of waves on the calculation of storm surges in the North Sea. They reported that taking the dependence of the drag coefficient on the sea state into account, it is possible to improve the storm surge predictions. Tolman (1990) studied the effect of currents on the wave field in applications with a relatively coarse space resolution.

In this work, we explore the dependence of the wave evolution on an inhomogeneous, unsteady current field in finite-depth waters and this at intermediate spatial resolution ($O(5 \text{ km})$). To this end the third-generation WAM model (Günther et al., 1994) was modified (Luo and Sclavo, 1997; Monbaliu et al, 1998) and it was implemented for applications in the North Sea. The hydrodynamic fields were computed by a tide/surge model and transferred off-line to the wave model. The main goal here is to investigate the sensitivity of the results at the local scale to the frequency of information exchange and to the source of boundary conditions in a loose one way coupled system.

2 The numerical models

2.1 The wave model

The wave model used is the third generation WAM *Cycle-4* model (Günther et al., 1994). The model solves an energy balance equation for the spectrum $F(f, \theta)$ as a function of the wave frequency, f , wave direction, θ , and the geographical position, \mathbf{x} , and time, t . The standard version of WAM propagates the energy over a calculational grid in Cartesian coordinates $\mathbf{x}(x, y)$ for small area applications or in spherical coordinates $\mathbf{x}(\phi, \lambda, r)$ for model applications over large areas as to take into account the swell propagation over great circles. For this work the last option is used. The WAM model permits the inclusion of a stationary current background and uses the relative frequency, σ , as a coordinate. Under these conditions, the energy transport equations solved in the WAM *Cycle-4* model code is equivalent to the action density transport equation. The transport equation for the evolution of the wave spectrum $F(t, \phi, \lambda, \sigma, \theta)$ then reads

$$\frac{\partial F}{\partial t} + (\cos \phi)^{-1} \frac{\partial}{\partial \phi} (\dot{\phi} \cos \phi F) + \frac{\partial}{\partial \lambda} (\dot{\lambda} F) + \sigma \frac{\partial}{\partial \sigma} \left(\dot{\sigma} \frac{F}{\sigma} \right) + \frac{\partial}{\partial \theta} (\dot{\theta} F) = S_{tot}, \quad (1)$$

where the expressions $\dot{\phi}$, $\dot{\lambda}$, $\dot{\sigma}$, and $\dot{\theta}$ represent the rate of change of energy in the space $(\phi, \lambda, \sigma, \theta)$. At the right hand side of (1), S_{tot} is the function representing the source and sink functions, and the conservative non-linear transfer of energy between wave components. In the present application, it includes wind input S_{in} , non-linear quadruplet wave-wave interactions S_{nl} , whitcapping dissipation S_{ds} and bottom friction dissipation S_{bf} . Standard values were used for the empirical coefficients in the source terms. The model has been used in a quasi-steady approach, assuming that the current and the water depth vary only slowly. A detailed description of the physics incorporated in WAM *Cycle-4* model and its numerical implementation can be found in Komen et al., (1994). Details on the improvements, alterations and additions for application in nearshore regions can be found in Luo and Sclavo (1997) and Monbaliu et al. (1998).

2.2 The tide/surge model

The hydrodynamic (u, v, η) fields are computed with a model based on the shallow water equations. The spherical coordinate expressions for this set of equation are (Washington and Parkinson, 1986)

$$\begin{aligned} \frac{\partial u}{\partial t} &+ \frac{u}{R \cos \phi} \frac{\partial u}{\partial \lambda} + \frac{v}{R} \frac{\partial u}{\partial \phi} - \frac{uv \tan \phi}{R} - 2\omega \sin \phi v \\ &= - \frac{g}{R \cos \phi} \frac{\partial \eta}{\partial \lambda} - \frac{1}{\rho R \cos \phi} \frac{\partial P_a}{\partial \lambda} - \frac{\tau_{b\lambda}}{\rho(h + \eta)} + \frac{\tau_{s\lambda}}{\rho(h + \eta)} \\ &+ A_h \left[\nabla^2 u + \frac{u}{R^2} (1 - \tan^2 \phi) - 2 \frac{\tan \phi}{\cos \phi} \frac{\partial v}{\partial \lambda} \right], \end{aligned} \quad (2)$$

$$\begin{aligned} \frac{\partial v}{\partial t} + \frac{u}{R \cos \phi} \frac{\partial v}{\partial \lambda} + \frac{v}{R} \frac{\partial v}{\partial \phi} - \frac{u^2 \tan \phi}{R} + 2\omega \sin \phi u \\ = - \frac{g}{R} \frac{\partial \eta}{\partial \phi} - \frac{1}{\rho R} \frac{\partial P_a}{\partial \phi} - \frac{\tau_{b\phi}}{\rho(h + \eta)} + \frac{\tau_{s\phi}}{\rho(h + \eta)} \\ + A_h \left[\nabla^2 v + \frac{v}{R^2} (1 - \tan^2 \phi) + 2 \frac{\tan \phi}{\cos \phi} \frac{\partial u}{\partial \lambda} \right], \end{aligned} \tag{3}$$

$$\frac{\partial \eta}{\partial t} + \frac{1}{R \cos \phi} \left[\frac{\partial}{\partial \lambda} ((h + \eta)u) + \frac{\partial}{\partial \phi} ((h + \eta)v \cos \phi) \right] = 0, \tag{4}$$

where (u, v) are the horizontal (λ, ϕ) components of the velocity, ρ the sea water density, g the acceleration due to the gravity, ω the angular speed of the earth's rotation, η the water elevation (with respect to mean sea level), h is the mean depth, P_a the atmospheric pressure, $(\tau_{b\lambda}, \tau_{b\phi})$ the bottom stress components due to friction, $(\tau_{s\lambda}, \tau_{s\phi})$ the surface stress components due to wind. A_h the depth averaged kinematic eddy viscosity, and ∇^2 denotes the horizontal Laplacian operator in spherical coordinates. Equations (2) and (3) are the vertically integrated momentum equations and equation (4) states the conservation of mass. The information concerning the numerics can be found in Yu (1993).

3 Model implementations

3.1 WAM model implementations

Three nested grid were used: one coarse grid of which the domain extends up to 70N (Figure 1) as to capture the swell generated outside but traveling into the region of interest; a local grid covering part of the Southern North Sea basin (Figure 2); and a high resolution grid which takes into account the most important details of the bathymetry near the Flemish coast (not shown). The emphasis in this study is on the results obtained for the local grid.

The spectrum $F(f, \theta)$ was discretized using 12 directions and 25 frequencies with the standard logarithmic distribution. Both the coupled and uncoupled versions of the WAM model were run over the same grid and the option for energy propagation in spherical coordinates was used for all runs.

From the time series of wave parameters calculated from buoy data we used the *significant wave height*,

$$H_s = 4\sqrt{m_0}, \tag{5}$$

and the *zero upcrossing period*,

$$T_{m02} = \sqrt{m_0/m_2}, \tag{6}$$

where

$$m_i = \int \int F(f, \theta) f^i df d\theta. \tag{7}$$

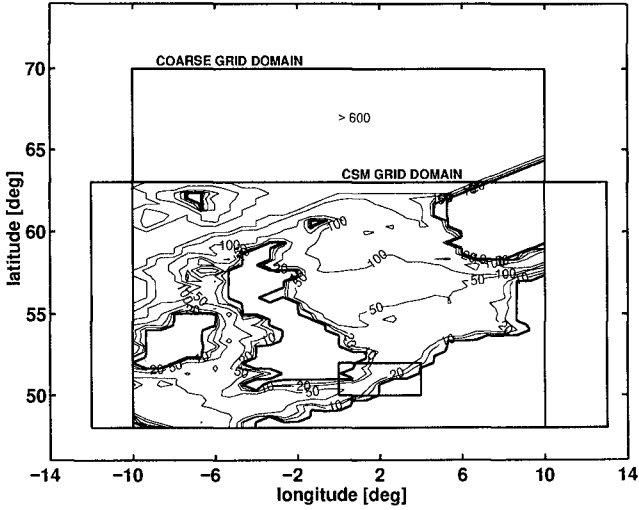


Figure 1: Coarse and CSM grid domain. The coarse grid bathymetry is included. Boundary condition for a nested local grid (region indicated by the square) are generated. Depth values are in meters.

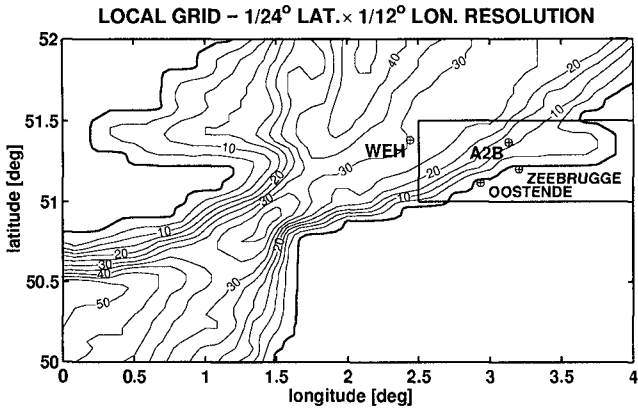


Figure 2: Local grid bathymetry with location indication of the WEH and A2B buoys. Boundary condition for a fine grid (region indicated by the square) are generated. Depth values are in meters.

Wind data are six-hourly winds for the North Sea region produced by UKMO (United Kingdom Meteorological Office). The wind data were interpolated onto the coarse grid points. This wind data set was then also used for the two nested grids, where they were interpolated internally in the WAM-model. Time interpolation was not used. Details concerning the different grids and integration time steps used are given in Table 1.

Table 1: Types, geographical coverage, resolution, and time step (advection and source terms) for each grid used.

GRID	AREA	RESOLUTION (LAT \times LON)	TIME STEP	
			Advection	Source
WAM MODEL (Type-A Grid)				
Coarse	48.0N - 70.0N 10.0W - 10.0E	$(1/3)^\circ \times (2/3)^\circ$	20 min	20 min
Local	50.0N - 52.0N 0.0E - 4.0E	$(1/24)^\circ \times (1/12)^\circ$	4 min	20 min
Fine	51.0N - 51.5N 2.5E - 4.0E	$(1/96)^\circ \times (1/96)^\circ$	30 sec	10 min
CSM Model (Type-C Grid)				
CSM	48.0N - 63.0N 12.0W - 13.0E	$(1/24)^\circ \times (1/12)^\circ$	10 min	-

3.2 Surge model implementation

The hydrodynamic fields were obtained from a Continental Shelf Model (CSM) which solved the set of equations (2)–(4) with a spatial coverage and resolution indicated in Table 1. The model was forced at the boundary with eight tidal constituent. No surge effect was taken into account. Current (u, v) and elevation (η) fields were generated on a Type-C grid. These fields were linearly interpolated to the local and fine WAM type-A grids. Note that η points from the CSM grid correspond to the local grid WAM points. For the coarse grid, the closest values of (u, v) were assigned to each wet point of the WAM grid. For the hydrodynamic data from 63°N to 70°N needed in the WAM coarse grid coupled run, the values at the 63°N points were taken.

4 Results

4.1 Introduction

The performance of coupled and uncoupled versions of the WAM was tested on a one-month period (February 1993) for the coarse and local grid. The fine grid version was run only for a 15-day period due to the high computational effort required.

In what follows, time series at the locations WEH (Westhinder) and A2B from both coupled and uncoupled WAM results are compared with the available buoy data. The sensitivity to 'coupled' information in the boundary conditions, and to the frequency of information exchange is addressed for the local grid application. The evolution of 1D-spectra and 2D-spectra in 'coupled' and 'uncoupled' mode are discussed.

4.2 Time series

Time series calculated by WAM at station WEH (30m depth) show a good agreement with buoy data, especially for significant wave height (H_s) values during high-wave events (see Figure 3). The small modulations visible in the buoy data at WEH seem well reproduced by the coupled version of WAM. However, the presence of some modulations in the uncoupled run results suggests that part of the modulations in the signal must come from wind variability. The bias for H_s in the coupled and uncoupled results is -0.072m and -0.143m, respectively. The intercomparison between results from coupled and uncoupled models show differences (coupled - uncoupled) in H_s smaller than 0.25m, with a mean difference of 0.02m. Modulations of $T_{m_{02}}$, corresponding to the dominant semidiurnal tide period, are quite clear in the buoy data (Figure 3). The importance of including the hydrodynamic fields is highlighted qualitatively by the good agreement between buoy data and WAM-coupled results for $T_{m_{02}}$. This is not directly reflected in the value for the bias for $T_{m_{02}}$, which were 0.032s for the coupled and 0.034s for the uncoupled run, respectively. The model results themselves showed differences up to 1.0s, with a mean difference of -0.15s.

In the more shallow A2B station (11m depth), overestimation of model results with respect to buoy data is observed, both in H_s and in $T_{m_{02}}$ (Figure 4). Although it is possible to reduce the observed differences by tuning of the empirical coefficient in the bottom friction term (see Luo and Monbaliu, 1994, Luo et al., 1996), this was not done since it was not considered important for the scope of this work. At this station, the bias was -0.128m and -0.116m for H_s and -0.846s and -0.965s for $T_{m_{02}}$ in the coupled and uncoupled mode, respectively. The importance of tidal modulations is again observed at this location and it is qualitatively well reproduced in the coupled run. Differences between coupled and uncoupled model results do not exceed 0.25m in H_s and 1.0s in $T_{m_{02}}$, whereas the mean difference in the H_s and $T_{m_{02}}$ value was 0.014m and -0.217s, respectively.

4.3 Sensitivity to boundary conditions

In order to explore the necessity to run in coupled mode on a coarse grid in order to supply good boundary conditions for a subsequent nested run, the application on the local grid was run once using boundary conditions from the coupled and once from the uncoupled coarse grid run. In both cases, results showed clearly the tidal modulation effect on $T_{m_{02}}$ (Figure 5a). The observed differences are small and most of the time do not exceed 5%, which seem to suggest that running the coarse grid

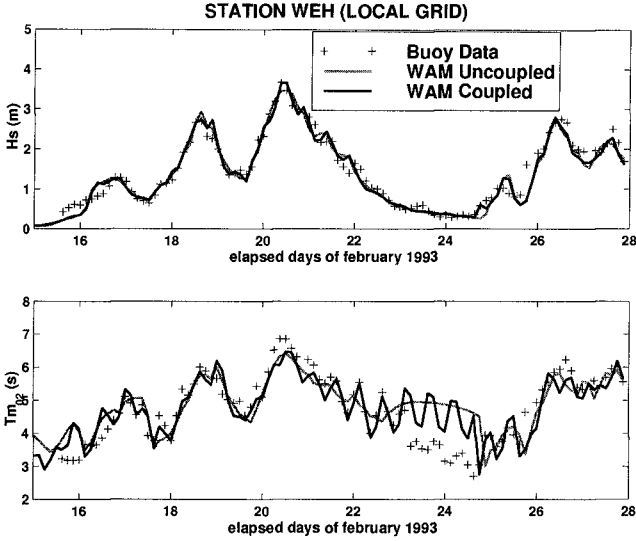


Figure 3: Time series of significant wave height (H_s) and zero upcrossing period (T_{m02}) at station WEH of the local grid.

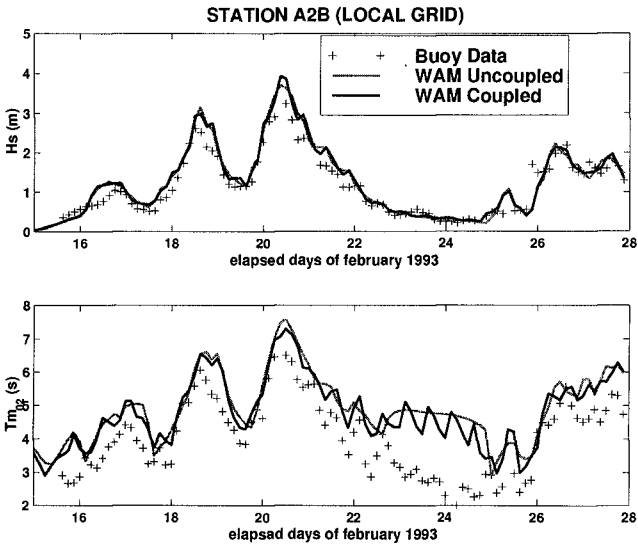


Figure 4: Time series of significant wave height (H_s) and zero upcrossing period (T_{m02}) at station A2B of the local grid.

application in coupled mode, does not have a dramatic influence on the local grid runs. Tide-induced modulations, at least on the space scales used here, are mainly a local effect.

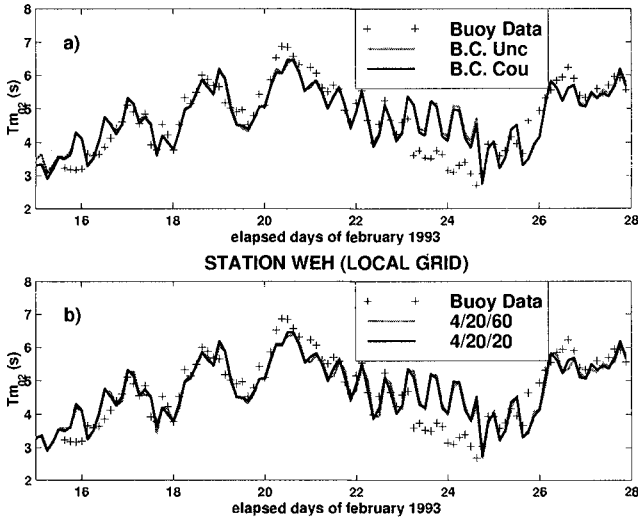


Figure 5: Time series showing the sensitivity to: (a) boundary conditions, and (b) information exchange of T_{m02} at station WEH.

4.4 Sensitivity to frequency of information exchange

In a coupled system, an important factor to define is the frequency of information transfer between model components. In this work, hydrodynamic fields were updated every 20 minutes (standard coupled mode), which seems suitable for the temporal scale of tide variability. In order to investigate the sensitivity of the model results to the frequency of information exchange, the coupled model on the local grid was also run with an update of the hydrodynamic fields every 60min. The results were compared with those of the standard run. The time series of T_{m02} presented in Figure 5b, show differences smaller than 5%. Some details in the modulation are missed. For this spatial scale and with current and depth fields which vary only slowly in time and space, the main variation in the spectral periods are well reproduced by the Doppler shift. As one can observe from the time series, the tidal modulations respond mainly to the semidiurnal tidal constituent M2. Further decrease of the frequency of information exchange will lead to increased loss of information.

4.5 Spectral evolution

In order to clarify the observed differences in the time series, it is appropriate to analyze how the spectral shape evolves in the presence of a current field. In Figure 6 we can observe the history of the 1D-spectra at station WEH as calculated by the coupled and uncoupled version of WAM. The frequency shifting effect is clearly observed as modulation with a period corresponding to the semidiurnal tidal constituent. These modulations are mainly observed at intermediate and low frequencies, where the effect is not masked by the wind variability.

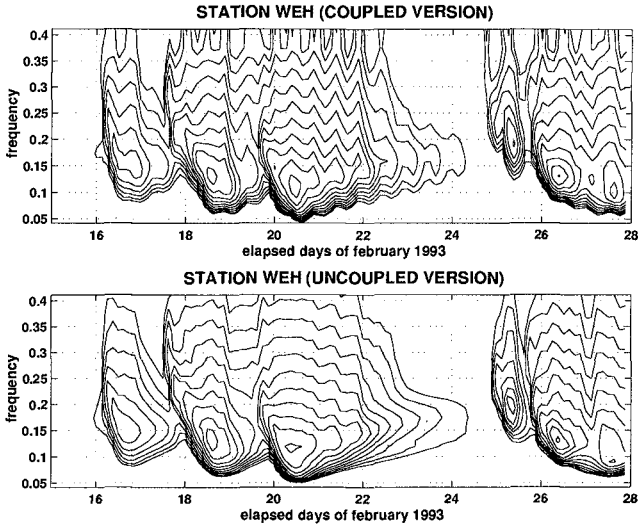


Figure 6: Evolution of the 1D spectra calculated by WAM coupled and uncoupled at location WEH. A logarithmic distribution of contour labels is used in both cases.

A definitive insight to clarify the differences in time series is the intercomparison of directional spectra. Hubbert and Wolf (1991) and Holthuijsen and Tolman (1991) studied the propagation of a wave spectrum across a current eddy. They found that the interaction with the current produce changes in the shape of the spectra (broadening and bimodality at some parts of the whirl) associated to the current induced refraction. The coupled runs produced slightly broader spectra than the uncoupled version, mainly at small angles between wave and current direction. An illustration of is given in Figure 7. Starting from almost the same spectrum (date: 93022515), it is possible to observe six hours later a fast growth of energy in the spectrum calculated by the coupled version. The fast growth is due to the wind, which remained relatively constant in magnitude and direction during that period. This produced a shifting of the mean wave direction toward the wind direction, almost 90 degrees from the original direction. Note that the WAM-model does not

have a linear 'Phillips' term in its wind input source function. It was not investigated in how far this is responsible for the lack of growth in the uncoupled version.

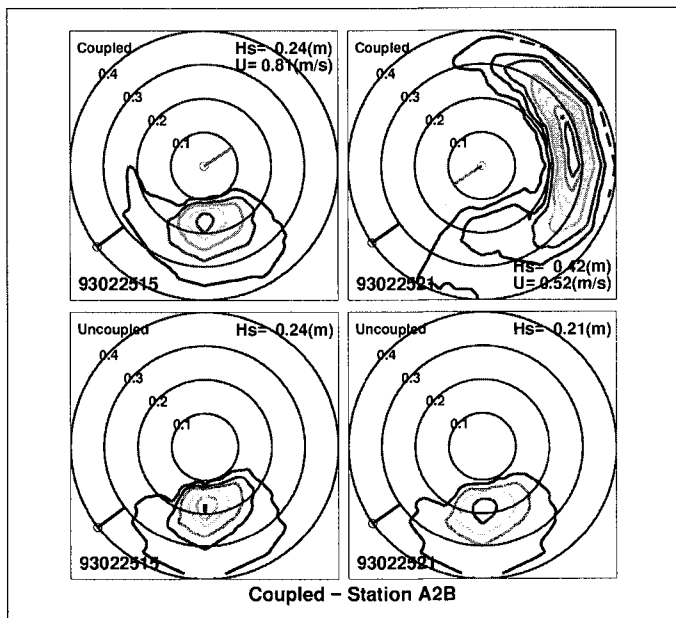


Figure 7: 2D spectra at station A2B calculated by WAM coupled and uncoupled. Significant wave height (H_s), wind direction (dark line) and date are always indicated. For coupled results, current magnitude (U) and current direction (light line) are indicated. The same contour labels were used in all figures (1, 5, and from 10 to 100% every 10% of $0.1\text{m}^2/\text{Hz}/\text{deg}$).

4.6 Further work

The fine grid bathymetry for the Flemish Coast is much more complicated than can be anticipated from Figure 2. Many sand banks more or less parallel with the coast are present. Their spatial scale is small such that they disappear from the local grid resolution. A fine grid wave model was nested in the local grid (see section 3.1). For the hydrodynamic fields linear interpolation from the CSM-grid (equal to the local wave model grid) to the fine grid was used. Comparison of time series at A2B from the local and fine grids showed only negligible differences. This is not unexpected since all the variability in the current field induced by the local bathymetry is not represented in the interpolated current field. If the details of the bathymetry are not taken into account in the calculation of the hydrodynamical variables, the directions of the waves and the currents become more and more perpendicular as

one approaches the coast. This produces a negligible effect of the currents on the characteristics of the wave field. The next logical step is therefore to use the same resolution for the hydrodynamic and the wave field calculations.

5 Conclusions

A modified version of the third generation spectral wave model WAM was used in a three level nested grid application to study the interaction of waves with currents. Numerical results from the local grid showed a very good agreement with buoy data. At the shallower station A2B some slight modulations (approximately $\pm 0.1\text{m}$) of the significant wave height were observed. Tidal effects were better visible as modulations on the wave period. These last effects were larger at the station WEH than at the station A2B.

Local grid results using boundary conditions from a coarse uncoupled run were qualitatively and quantitatively as good as the results considering boundary information from a coupled coarse run. This indicates that the results in the local grid are not sensitive to 'coupled' or 'uncoupled' boundary information. The results also do not seem very sensitive to the update frequency (from 20 to 60min) of the hydrodynamic information. This means that at least for this local grid application, currents and water depths vary slowly and that the doppler shift reproduces to a large extent the hydrodynamic interactions.

Tidal modulations with a period corresponding to the semidiurnal tidal constituent were observed in all the frequency components of the spectra. The directional spectra computed by the coupled version of WAM had a broader energy distribution and a more rapid energy growth was observed in changing wind conditions.

The negligible differences between local and fine grid results were attributed to a lack of spatial resolution in the hydrodynamic field. The next logical step is therefore to use the same spatial resolution for the wave and for the hydrodynamic calculations.

Acknowledgments

The buoy data were provided by AWK of the Ministry of the Flemish Community. This study is carried out with financial support from the PROMISE project under the EC-MAST III PROGRAMME, contract MAS3 CT 9500025.

References

- Günther, H., S. Hasselmann, and P.A.E.M. Janssen, 1994: User manual of the WAM Cycle 4. Report nr. 4, Hamburg.
- Graber, H.C., and O.S. Madsen, 1988: A finite-depth wind-wave model. Part I. Model description. *J. Phys. Oceanogr.* **18**, 1465-1483.

- Hubbert, K.P., and J. Wolf, 1991: Numerical investigation of depth and current refraction of waves. *J. Geophys. Res.*, **96**, 2737–2748.
- Holthuijsen, L., and H.L. Tolman, 1991: Effects of the Gulf Stream on ocean waves. *J. Geophys. Res.*, **96**, 12755–12771.
- Jonsson, I.G., 1990: Wave–current interactions. In B. Le Mehaute and D.M. Hanes (Eds.), *The Sea*, Ocean Engineering Science, Vol 9(A), p65–120. Wiley, New York.
- Komen, G.J., L. Cavaleri, M. Donelan, K. Hasselmann, S. Hasselmann, and P.A.E.M. Janssen, 1994: *Dynamics and modelling of ocean waves*. Cambridge University Press.
- Luo, W., and J. Monbaliu, 1994: Effects of the bottom friction formulation on the energy balance for gravity waves in shallow water. *J. Geophys. Res.*, **99**, 18501–18511.
- Luo, W., J. Monbaliu, and J. Berlamont, 1996: Bottom friction dissipation in the Belgian coastal region. *Proc. 25th Int. Conf. Coastal Eng.*, Florida, 836–849.
- Luo, W., and M. Sclavo, 1997: Improvement of the third generation WAM model (Cycle 4) for applications in nearshore regions. Internal report no. 116, Proudman Oceanographic Laboratory.
- Monbaliu, J., R. Padilla, P. Osuna, R. Flather, J. Hargreaves, J.C. Carretero, S. Espinar, and H. Günther, 1998: A shallow water version of the WAM spectral wave model. Report nr. 52, Proudman Oceanographic Laboratory. *To be published*.
- Mastenbroek, C., G. Burgers, and P.A.E.M. Janssen, 1993: The dynamical coupling of a wave model and a storm surge model through the atmospheric boundary layer. *J. Phys. Oceanogr.*, **23**, 1856–1866.
- Mei, C.C., S. Fan, and K. Jin, 1997: Resuspension and transport of fine sediments by waves. *J. Geophys. Res.*, **102**, 15807–15821.
- Shemdin, O.H., S.V. Hsiao, H.E. Carlson, K. Hasselmann, and K. Schulze, 1980: Mechanisms of wave transformation in finite-depth water. *J. Geophys. Res.* **85**, 5012–5018.
- Tolman, H.L., 1990: Wind wave propagation in tidal seas. *Communications on hydraulic and geotechnical engineering*, Delft University of Technology. Report nr. 90–1.
- Washington, W.M., and C.L. Parkinson, 1986: *An introduction to three-dimensional climate modelling*. Oxford University Press.
- Yu, C.S., 1993: Modelling Shelf Sea Dynamics, Ph.D. thesis, Department of Civil Engineering, K.U.Leuven, Belgium.